Lattice QCD Calculation of $\pi^0 \to e^+e^-$ Decay

Norman Christ,[1] Xu Feng,[2] Luchang Jin,[3] Cheng Tu,[3] and Yidi Zhao[1]
[1]*Physics Department, Columbia University, New York, New York 10027, USA*
[2]*School of Physics, Peking University, Beijing 100871, China; Collaborative Innovation Center of Quantum Matter, Beijing 100871, China; and Center for High Energy Physics, Peking University, Beijing 100871, China*
[3]*Physics Department, University of Connecticut, Storrs, Connecticut 06269-3046, USA*

(Received 24 August 2022; accepted 11 April 2023; published 12 May 2023)

We extend the application of lattice QCD to the two-photon-mediated, order α^2 rare decay $\pi^0 \to e^+e^-$. By combining Minkowski- and Euclidean-space methods we are able to calculate the complex amplitude describing this decay directly from the underlying theories (QCD and QED) which predict this decay. The leading connected and disconnected diagrams are considered; a continuum limit is evaluated and the systematic errors are estimated. We find $\mathrm{Re}\mathcal{A} = 18.60(1.19)(1.05)$ eV, $\mathrm{Im}\mathcal{A} = 32.59(1.50)(1.65)$ eV, a more accurate value for the ratio $(\mathrm{Re}\mathcal{A}/\mathrm{Im}\mathcal{A}) = 0.571(10)(4)$, and a result for the partial width $\Gamma(\pi^0 \to \gamma\gamma) = 6.60(0.61)(0.67)$ eV. Here the first errors are statistical and the second systematic. This calculation is the first step in determining the more challenging, two-photon-mediated decay amplitude that contributes to the rare decay $K \to \mu^+\mu^-$.

DOI: 10.1103/PhysRevLett.130.191901

Introduction.—The rare decay $\pi^0 \to e^+e^-$ involves a combination of the strong and electromagnetic interactions and is significantly suppressed by a factor of $(m_e/M_\pi)^2$ that results from the kinematics of the decay and the chiral symmetry of the electromagnetic coupling of the electron. This large suppression increases the sensitivity of this process to new chirally asymmetric interactions of the quarks and leptons and is an interesting target for a high-precision comparison between experiment and the predictions of the standard model.

The $\pi^0 \to e^+e^-$ branching ratio has been measured to 4% accuracy in the KTeV experiment [1], giving $B(\pi^0 \to e^+e^-) = 6.86(27)_{\mathrm{stat}}(23)_{\mathrm{syst}} \times 10^{-8}$ after radiative corrections discussed below have been performed. This can be compared with the recent precise standard model prediction [2] of $6.25(3) \times 10^{-8}$. Reference [2] provides extensive references to earlier theoretical results, which also typically lie below the experimental value. This 1.7σ discrepancy adds to the interest in this process and provides motivation to pursue independent theoretical techniques such as those of lattice QCD.

Recent advances in the methods of lattice QCD allow the calculation of increasingly complex processes which involve both QCD and QED. While initially motivated by the calculation of the light-by-light scattering process which contributes to the anomalous magnetic moment, $g_\mu - 2$, of the muon [3,4], these methods can be applied to other processes where an *ab initio* lattice QCD result would be of value. In contrast with light-by-light scattering entering $g_\mu - 2$ which can be computed using Euclidean-space methods, $\pi^0 \to e^+e^-$ is inherently a Minkowski process with a complex amplitude resulting from physical time evolution. Here we develop a method that allows us to deal with such a process using lattice QCD. We note that this method may also allow a lattice QCD calculation of the two-photon-exchange amplitude needed for a test of the standard model predictions in the rare flavor-changing neutral current decay $K_L \to \mu^+\mu^-$.

To leading order the $\pi^0 \to e^+e^-$ decay is mediated by a two-photon intermediate state as shown in Fig. 1. The decay amplitude $\mathcal{A}$ is complex with an imaginary part determined by the optical theorem, giving the well-known unitary bound for the $\pi^0 \to e^+e^-$ branching ratio [5]. We will use lattice QCD to compute both the real and imaginary parts of $\mathcal{A}$ using a treatment of QED without power-law finite-volume errors. Thus, our result for the imaginary part provides an improved calculation of the partial width $\pi^0 \to \gamma\gamma$ with finite volume errors that vanish exponentially with increasing volume, without the constraint to use photon momenta that obey quantization conditions related to the volume used in the lattice QCD calculation [6]. (Preliminary results from these methods appear in Refs. [7–10].)

As is conventional, a comparison between theory and experiment for the $\pi^0 \to e^+e^-$ decay is made after the

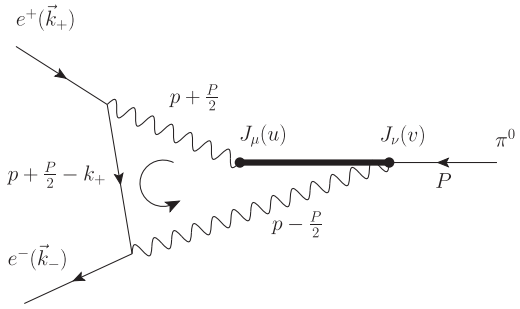

FIG. 1. The leading order Feynman diagram for $\pi^0 \to e^+e^-$ decay. Here we do not show the quark structure of the QCD portion of the amplitude which is represented by the heavy line. However, the two hadronic electromagnetic currents are distinguished and their time ordering suggested.

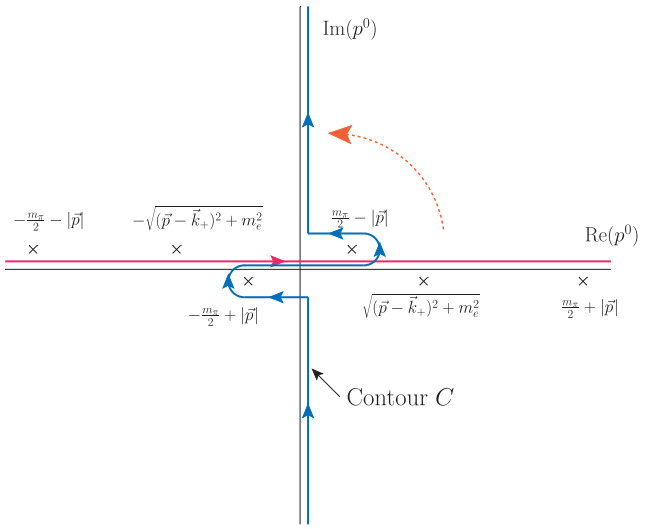

FIG. 2. The deformed p^0 integration contour. The six crosses locate the six poles of the integrand in Eq. (1).

conventional $O(\alpha)$ radiative corrections have been performed. These corrections [11,12] require a two-loop calculation in which the zeroth-order $\pi^0 \to e^+e^-$ decay is not approximated as pointlike. We follow Refs. [11,12] to remove these radiative effects from the experimental results, obtaining $B(\pi^0 \to e^+e^-) = 6.86(27)_{\mathrm{stat}}(23)_{\mathrm{syst}} \times 10^{-8}$. This corrected experimental result can be compared with our lattice calculation which also does not include these effects. These corrections depend on the low-energy constant $\chi^{(r)} = 4.5(3)$ (defined at the scale $\mu = 770$ MeV) which was determined recursively from the experimental result with these corrections removed.

Computational strategy.—We start with the Minkowski-space expression for the decay amplitude:

$$\mathcal{A} = e^4 \int d^4w \left\langle 0|T\left\{J_\mu\left(\frac{w}{2}\right)J_\nu\left(-\frac{w}{2}\right)\right\}|\pi^0\right\rangle \int \frac{d^4p}{(2\pi)^4} e^{-ip\cdot w}\left[\frac{g_{\mu\mu'}}{\left(p+\frac{P}{2}\right)^2 - i\epsilon}\right]\left[\frac{g_{\nu\nu'}}{\left(p-\frac{P}{2}\right)^2 - i\epsilon}\right]\bar{u}(k_-,h)\gamma_{\mu'} \times \left[\frac{\gamma\cdot(p+\frac{P}{2}-k_+)+m_e}{(p+\frac{P}{2}-k_+)^2+m_e^2-i\epsilon}\right]\gamma_{\nu'}v(k_+,h), \tag{1}$$

where $w = u - v$ is the relative space-time position of the two electromagnetic currents, $P = (\vec{0}, M_\pi)$ is the four-momentum of initial pion, and $h = \pm\frac{1}{2}$ is the helicity of the electron on which $\mathcal{A}$ does not depend. Note that we have integrated out their average position $(u+v)/2$ and removed the resulting δ function that imposes total energy and momentum conservation. The Minkowski metric tensor $g_{\mu\mu'} = \mathrm{diag}(-1,1,1,1)$.

A direct Euclidean-space calculation of the hadronic matrix element in Eq. (1) using lattice methods is feasible if we Wick rotate the w^0 contour by replacing the real variable w^0 with the product $e^{-i\phi}w_0$ and increase ϕ from 0 to $\pi/2$ while keeping w_0 real, thereby making w^0 a Euclidean time. At the same time, the p^0 contour must also be rotated so that the exponent ip^0w^0 in Eq. (1) remains purely imaginary as $|p^0| \to \infty$. Because of the existence of the two-photon intermediate state whose energy may be lower than the energy of initial pion state, the rotated p^0 contour cannot simply follow the imaginary axis. Instead the p^0 contour must be distorted as in Fig. 2 to avoid the poles which cross the imaginary axis when the energy of the two-photon intermediate state is lower than the pion mass, $2|\vec{p}| < M_\pi$.

This choice of contour guarantees that the p^0 integral will converge. However, once the variable w^0 has become imaginary, the factor $e^{-ip\cdot w}$ will grow exponentially with $|w^0|$ for the real values of p^0 that appear for the contour of Fig. 2. Fortunately, the Euclidean-space hadronic matrix element $H_{\mu\nu}(w)$ will compensate for this behavior, so that both the p^0 and w^0 integrations are convergent. The dependence of the hadronic matrix element on w^0 can be determined by inserting a complete set of intermediate states between the two electromagnetic currents in the hadronic matrix element $\langle 0|T\{J_\mu(w/2)J_\nu[-(w/2)]\}|\pi^0\rangle_E$:

$$\sum_n \langle 0|J_\mu\left(\frac{\vec{w}}{2},0\right)|n\rangle\langle n|J_\nu\left(-\frac{\vec{w}}{2},0\right)|\pi^0\rangle e^{|w^0|(M_\pi/2-E_n)}. \tag{2}$$

The lightest intermediate state is the two-pion state with $E_n = 2M_\pi$. Thus, this Euclidean-space hadronic matrix element will decay as $\exp(-3M_\pi|w^0|/2)$ for large $|w^0|$. This large-$|w^0|$ falloff is sufficient to overcome the $\exp(|w^0|M_\pi/2)$ growth due to the p^0 contour in Fig. 2.

We can write the analytic expression for the decay amplitude after contour deformation as follows:

$$\mathcal{A} = \int d^4w L_{\mu\nu}(w) H_{\mu\nu}(w), \tag{3}$$

$$\begin{aligned} EL_{\mu\nu}(w) = e^4 \int \frac{d^3p}{(2\pi)^4} \int_C dp^0 e^{-i\vec{p}\cdot\vec{w}} e^{+p^0 w^0} \\ \times \left[\frac{\tilde{g}_{\mu\mu'}}{(p+\frac{P}{2})^2 - i\epsilon}\right] \left[\frac{\tilde{g}_{\nu\nu'}}{(p-\frac{P}{2})^2 - i\epsilon}\right] \bar{u}\left(k_-, \frac{1}{2}\right)\gamma_{\mu'} \\ \times \left[\frac{\gamma\cdot(p+\frac{P}{2}-k_+)+m_e}{(p+\frac{P}{2}-k_+)^2+m_e^2-i\epsilon}\right]\gamma_{\nu'} v\left(k_+, \frac{1}{2}\right), \end{aligned} \tag{4}$$

$$H_{\mu\nu}(w) = \langle 0|T\left\{J_\mu\left(\frac{w}{2}\right)J_\nu\left(-\frac{w}{2}\right)\right\}|\pi^0\rangle_E, \tag{5}$$

where $\tilde{g}_{\mu\mu'} = \mathrm{diag}(i,1,1,1)$ is introduced to connect the Minkowski conventions for the electromagnetic currents in $L_{\mu\nu}$ with the Euclidean conventions used in the hadronic matrix element. Note that the amplitude $\mathcal{A}$ is not altered by these changes of contour and remains complex with real and imaginary parts which can be computed from the Euclidean-space amplitude in Eq. (5).

The leptonic factor $L_{\mu\nu}$ is evaluated by performing the p^0 integral using Cauchy's theorem, resulting in a three-dimensional integral over $\vec{p}$. When integrated over $|\vec{p}|$ the singular factor $[1/(|\vec{p}| - M_\pi/2 - i\epsilon)]$ gives both real and imaginary parts. Recognizing that the integral is independent of the direction of the outgoing positron momentum $\vec{k}_+$ allows us to average over this direction. Here we present the result for the spatial components, writing $L_{ij}(w) = L(w^0, |\vec{w}|)\epsilon_{ijk}w^k/|\vec{w}|^2$, with

$$L^{\mathrm{Im}}(w^0, |\vec{w}|) = 2\pi\alpha^2 \frac{m_e}{M_\pi^2}\frac{1}{\beta}\ln\left(\frac{1+\beta}{1-\beta}\right) F\left(\frac{M_\pi}{2}|\vec{w}|\right), \tag{6}$$

$$\begin{aligned} L^{\mathrm{Re}}(w^0, |\vec{w}|) = 4m_e\alpha^2 \Bigg\{ \ln\left(\frac{1+\beta}{1-\beta}\right)\mathcal{P}\int_0^\infty \frac{d|\vec{p}|}{M_\pi^2\beta} \frac{e^{-|\vec{p}||w^0|}}{\left(\vec{p}^2 - \frac{M_\pi}{2}\right)^2} F(|\vec{p}||\vec{w}|)\left[\frac{M_\pi}{2}\sinh\left(\frac{M_\pi}{2}|w^0|\right) + |\vec{p}|\cosh\left(\frac{M_\pi}{2}|w^0|\right)\right] \\ + \int_0^\infty d|\vec{p}| d\cos\theta \frac{e^{-E_e(|\vec{k}_+|,|\vec{p}|,\theta)|w^0|}F(|\vec{p}||\vec{w}|)}{E_e(|\vec{k}_+|,|\vec{p}|,\theta)(-M_\pi + 2|\vec{k}_+|\cos\theta)(M_\pi + 2|\vec{k}_+|\cos\theta)}\Bigg\}. \end{aligned} \tag{7}$$

Here $\beta = \sqrt{1-4m_e^2/M_\pi^2}$, $F(x) = \cos(x) - \sin(x)/x$, and $E_e(k,p,\theta) = \sqrt{k^2+p^2-2pk\cos(\theta)+m_e^2}$. We then evaluate the leptonic factor $L_{\mu\nu}$ as a two-dimensional numerical integral, requiring that the integration error lies below 0.001%. The result is tabulated as a function of w^0 and $|\vec{w}|$. We evaluate the four-dimensional integral over w in Eq. (3) as a sum over lattice points with the values of $L_{\mu\nu}(w)$ obtained from this table by linear interpolation. We specify the normalization conventions for the amplitude $\mathcal{A}$ by the relation $\Gamma_{\pi^0\to e^+e^-} = \beta|\mathcal{A}|^2/(8\pi M_\pi)$.

Hadronic matrix element.—The hadronic matrix element $H_{\mu\nu}$ in Eq. (5) can be calculated from the three-point function:

$$\begin{aligned} &\langle 0|T\{J_\mu(x)J_\nu(0)\}|\pi\rangle \\ &= \frac{Z_V^2}{N_\pi}\lim_{t_\pi\to-\infty} e^{M_\pi|t_\pi|}\langle J_\mu(x)J_\nu(0)\pi^0(t_\pi)\rangle^{\mathrm{lat}}, \end{aligned} \tag{8}$$

which can be computed using lattice QCD. It is only in this evaluation of $H_{\mu\nu}$ that a finite volume is introduced. Since this Euclidean-space amplitude involves no massless particles, all finite-volume errors will decrease exponentially in the linear size of the volume.

The factor Z_V renormalizes the nonconserved, local current used in the lattice calculation of the right-hand side of Eq. (8). The factor N_π is obtained from the π^0 two-point function and compensates for the normalization of the pion interpolating operator $\pi^0(t_\pi)$. We use a Coulomb-gauge-fixed wall source for this operator.

The two diagrams needed to evaluate this three-point function are shown in Fig. 3. The first is connected and can be constructed from two wall-source propagators and one point-source propagator. The two electromagnetic currents must be located sufficiently far from the pion interpolating operator so that contamination from states more energetic than the pion can be neglected. We require the pion source at t_π to be separated from the closer current by a fixed time Δt_π. We view our lattice as a one-dimensional torus in time with extent T and identify a direction of increasing time. We define the time locations of current operators as $t_>$ and $t_<$, where the $t_>$ is later than $t_<$ by a time shorter than $T/2$. We average the case where t_π is Δt_π earlier than $t_<$ and the case where t_π is Δt_π time later than $t_>$.

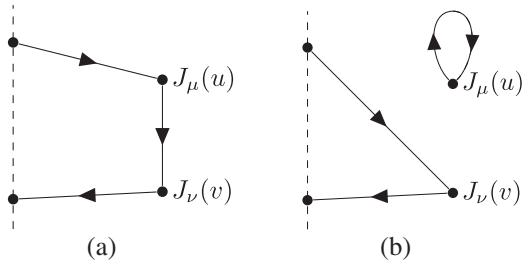

FIG. 3. The quark propagator contractions needed for the hadronic three-point function given in Eq. (8). The dashed line locates the wall-source pion interpolating operator. (a) Connected. (b) Disconnected.

The second diagram is quark-line disconnected. Such disconnected diagrams typically involve large statistical noise and are difficult to calculate. In our calculation, we use for the quark loop shown in Fig. 3(b) the results for $\mathrm{Tr}[D^{-1}(x,x)\gamma_\mu]$ computed using all-to-all propagators computed with randomly displaced, 3^4 grid sources from the RBC and UKQCD Collaborations' calculation of the disconnected contribution to the hadronic vacuum polarization component of $g_\mu - 2$ [13]. As shown in Table III, we determine this disconnected amplitude with a statistical error of 60%.

The hadronic matrix element is calculated on four ensembles, whose parameters are listed in Table I. All ensembles use Möbius domain wall fermions, which achieve good chiral symmetry with a much smaller size in the fifth dimension than required by the conventional domain wall fermion action. All ensembles use the Iwasaki gauge action. The 24ID, 32ID, and 32IDF ensembles use the dislocation suppressing determinant ratio action to reduce chiral symmetry breaking effects. For every configuration, we have 1024 or 2048 point-source propagators with randomly distributed sources and Coulomb-gauge-fixed wall-source propagators with sources on every time slice.

Results.—The calculated real and imaginary parts of the amplitude are listed in Table II and plotted in Fig. 4.

TABLE I. Table of gauge-field ensembles, generated by the RBC and UKQCD Collaborations [14]. Here $\Delta_{\mathrm{configs}}$, N_{configs}, and $N_{\mathrm{pt\ srcs}}$ are the separation in molecular dynamics time between measurements, the number of configurations, and the number of point sources per configuration used, respectively.

	24ID	32ID	32IDF	48I	64I
a^{-1} (GeV)	0.98	0.98	1.37	1.73	2.36
M_π (MeV)	137	137	141	139	139
Z_V	0.7267(4)	0.7260(2)	0.683(1)	0.7108(3)	0.7429(1)
$\Delta_{\mathrm{configs}}$	10	10	10	10	20
N_{configs}	47	47	61	32	49
$N_{\mathrm{pt\ srcs}}$	1024	2048	1024	1024	1024
Δt_π	10	10	14	16	22

TABLE II. The lattice and experimental results for the real and imaginary parts of the decay amplitude in eV and their ratios. The error in parenthesis is statistical or experimental.

Source	Im$\mathcal{A}$ (eV)	Re$\mathcal{A}$ (eV)	Re$\mathcal{A}$/Im$\mathcal{A}$
24ID	38.58(54)	23.06(40)	0.5976(24)
32ID	39.80(36)	23.88(29)	0.6000(20)
32IDF	36.17(47)	21.48(33)	0.5939(22)
48I	35.19(81)	20.70(66)	0.5881(52)
64I	33.99(54)	19.73(42)	0.5803(35)
Experiment	35.45(27)	24.1(2.0)	0.68(6)

In Table II the experimental value for the imaginary part is evaluated using the optical theorem and the experimental pion lifetime; the experimental real part is obtained by subtracting the imaginary part contribution from the experimental decay rate, with radiative corrections. In the table

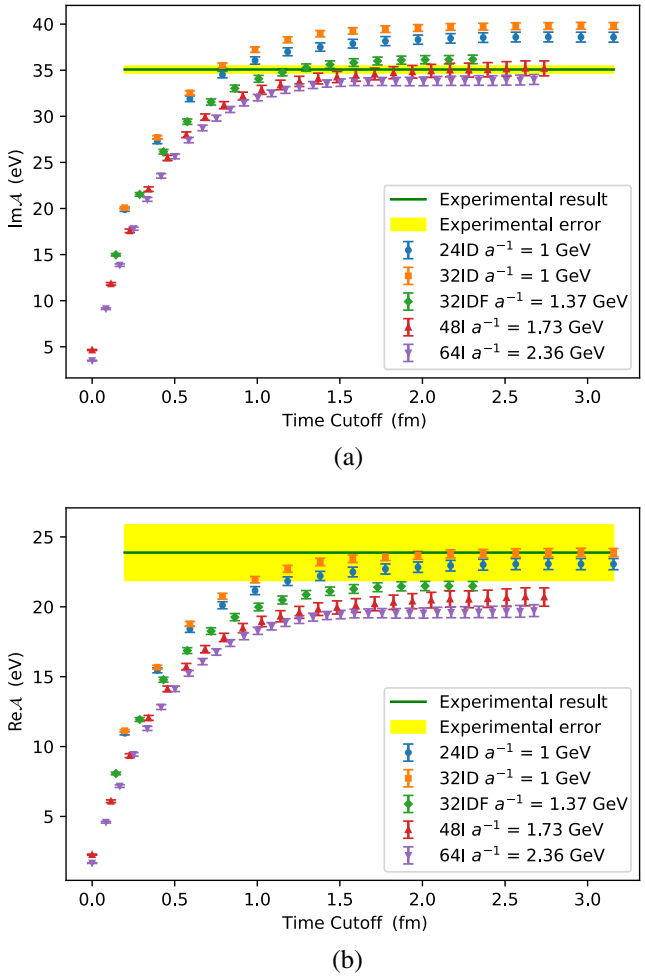

FIG. 4. The amplitude $\mathcal{A}$ plotted as a function of $t_{\mathrm{max}} < T/2$. Here we shift and/or reflect the time coordinate so that $t_\pi = 0$ and the earliest current is at Δt_π. We then sum over the time of the later current between the times Δt_π and t_{max}. (a) Imaginary part. (b) Real part.

TABLE III. The contribution to amplitude from connected and disconnected diagrams for the 24ID ensemble. The errors in parentheses are statistical.

Diagram	Im$\mathcal{A}$ (eV)	Re$\mathcal{A}$ (eV)	Re$\mathcal{A}$/Im$\mathcal{A}$
Connected	38.58(54)	23.06(40)	0.5976(24)
Disconnected	−1.1(54)	−0.62(40)	+0.0012(30)

and plot only the contribution from the connected diagram is included. The contribution from the disconnected diagram is treated as a source of systematic error. The disconnected diagram is calculated for the 24ID ensemble and the result shown in Table III.

We use the continuum limit extrapolated from the 48I and the 64I ensembles as shown in Fig. 5 as our final result. Estimates of the dominant systematic errors are given in Table IV. The finite-volume error is estimated from the difference between the 24ID and 32ID results, assuming that it behaves as $e^{-M_\pi L}$, where L is the linear lattice size. The error from omitting disconnected diagrams is estimated

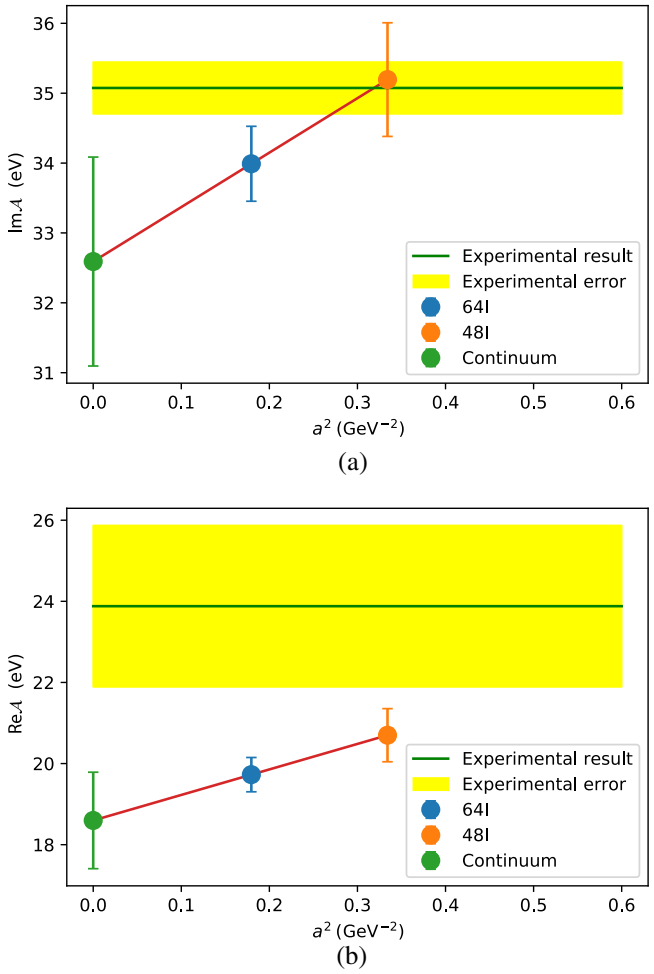

FIG. 5. Continuum extrapolation showing statistical errors. (a) Imaginary part. (b) Real part.

TABLE IV. Systematic error estimates.

Sources	Im$\mathcal{A}$ (eV)	Re$\mathcal{A}$ (eV)	Re$\mathcal{A}$/Im$\mathcal{A}$
Finite volume	1.33	0.89	0.0026
Disconnected diagram	0.94	0.50	0.0029
Continuum extrapolation	0.28	0.22	0.0018
Unphysical light m_{sea}	0.06	0.03	0.0
Total systematic error	1.65	1.05	0.0043

by comparing the connected and disconnected contributions for the 24ID ensemble listed in Table III. The discretization error remaining after our linear $a^2 \to 0$ extrapolation is estimated by introducing a hypothetical a^4 term which is parametrized as $(ma)^2$ times the a^2 term found in our linear fit. We interpret the mass m as giving the scale that is responsible for these errors. We choose $m = 770$ MeV, the ρ mass, subtract this hypothesized a^4 contribution from the data, and take the change in the resulting $a^2 \to 0$ limit as the error. The 48I and 64I light valence quark masses are physical but the light sea quarks are heavier than physical giving an error estimated in chiral perturbation theory.

Our final results are $\text{Im}\mathcal{A} = 32.59(1.50)_{\text{stat}}(1.65)_{\text{syst}}$ eV, $\text{Re}\mathcal{A} = 18.60(1.19)_{\text{stat}}(1.05)_{\text{syst}}$ eV, and

$$\frac{\text{Re}\mathcal{A}}{\text{Im}\mathcal{A}} = 0.571(10)_{\text{stat}}(4)_{\text{syst}}. \tag{9}$$

The smaller error on this ratio results from statistical correlations and our method of estimating the systematic errors. We can combine our more accurate result for this ratio with the experimental result for the decay width $\Gamma(\pi^0 \to \gamma\gamma)$ to obtain more accurate values for the real part of the decay amplitude and the branching ratio [15]:

$$\begin{aligned} \text{Re}\mathcal{A} &= 20.2(0.4)_{\text{stat}}(0.1)_{\text{syst}}(0.2)_{\text{expt}}\ \text{eV}, \\ B(\pi^0 \to e^+e^-) &= 6.22(0.05)_{\text{stat}}(0.02)_{\text{syst}}(0.002)_{\text{expt}} \times 10^{-8}. \end{aligned} \tag{10}$$

The error labeled "expt" arises from the error on the measured $\pi^0 \to \gamma\gamma$ decay. This result for the branching ratio is 1.8σ below the experimental value [1] $B(\pi^0 \to e^+e^-)_{\text{expt}} = 6.86(27)_{\text{stat}}(23)_{\text{syst}} \times 10^{-8}$, from which radiative corrections have been removed.

Finally, we can use our result for the imaginary part of $\mathcal{A}$ to determine a lattice QCD prediction for the decay width $\Gamma(\pi^0 \to \gamma\gamma) = 6.60(0.61)_{\text{stat}}(0.67)_{\text{syst}}$ eV to be compared with the experimental result [16] $\Gamma(\pi^0 \to \gamma\gamma) = 7.802(0.052)_{\text{stat}}(0.105)_{\text{syst}}$ eV. This new lattice QCD result is computed with physical quark masses, contains finite-volume errors which are suppressed exponentially in the

linear extent of the lattice, and can be viewed as a refinement of earlier lattice results [17,18].

Conclusion and outlook.—We have applied a combination of covariant Feynman perturbation theory and lattice QCD to calculate the complex amplitude describing the decay $\pi^0 \to e^+e^-$. Our result for this decay branching ratio (which depends on the well-determined ratio $\mathrm{Re}\mathcal{A}/\mathrm{Im}\mathcal{A}$) is accurate at the percent level and follows the pattern of previous theoretical results lying below the experimental value. Our method for combining lattice QCD with photon and lepton propagators extends techniques developed to calculate the hadronic light-by-light scattering contribution to $g_\mu - 2$ and holds promise for the eventual calculation of the two-photon-exchange contribution to the rare decay $K_L \to \mu^+\mu^-$.

We would like to thank P. Sanchez and P. Masjuan as well as A. Soni for a valuable suggestion and our other RBC and UKQCD collaborators for helpful discussions and support. The calculations reported here were carried out on facilities of the USQCD Collaboration funded by the Office of Science of the U.S. Department of Energy. These calculations used gauge configurations and propagators created using resources of the Argonne Leadership Computing Facility, which is a U.S. DOE Office of Science User Facility supported under Contract No. DE-AC02-06CH11357. N. C. and Y. Z. were supported in part by U.S. DOE Grant No. DE-SC0011941. X. F. was supported in part by NSFC of China under Grants No. 12125501, No. 12070131001, and No. 12141501, and National Key Research and Development Program of China under Grant No. 2020YFA0406400. L. J. acknowledges support by U.S. DOE Office of Science Early Career Award No. DE-SC0021147 and U.S. DOE Award No. DE-SC0010339.

[1] E. Abouzaid *et al.* (KTeV Collaboration), Measurement of the rare decay $\pi^0 \to e^+e^-$, Phys. Rev. D **75**, 012004 (2007).
[2] M. Hoferichter, B.-L. Hoid, B. Kubis, and J. Lüdtke, Improved Standard-Model Prediction for $\pi^0 \to e^+e^-$, Phys. Rev. Lett. **128**, 172004 (2022).
[3] T. Blum, N. Christ, M. Hayakawa, T. Izubuchi, L. Jin, and C. Lehner, Lattice calculation of hadronic light-by-light contribution to the muon anomalous magnetic moment, Phys. Rev. D **93**, 014503 (2016).
[4] J. Green, N. Asmussen, O. Gryniuk, G. von Hippel, H. B. Meyer, A. Nyffeler, and V. Pascalutsa, Direct calculation of hadronic light-by-light scattering, Proc. Sci. LATTICE2015 (**2016**) 109 [arXiv:1510.08384].
[5] S. Berman and D. Geffen, The electromagnetic structure and alternative decay modes of the π^0, Nuovo Cimento **18**, 1192 (1960).
[6] H. B. Meyer, Lattice QCD and the two-photon decay of the neutral pion, Eur. Phys. J. A **49**, 84 (2013).
[7] N. H. Christ, X. Feng, L. Jin, C. Tu, and Y. Zhao, Lattice QCD calculation of the two-photon contributions to $K_L \to \mu^+\mu^-$ and $\pi^0 \to e^+e^-$ decays, Proc. Sci. LATTICE2019 (**2020**) 128.
[8] N. H. Christ, X. Feng, L. Jin, C. Tu, and Y. Zhao, Calculating the two-photon contribution to $\pi^0 \to e^+e^-$ decay amplitude, Proc. Sci. LATTICE2019 (**2020**) 097 [arXiv:2001.05642].
[9] Y. Meng, X. Feng, C. Liu, T. Wang, and Z. Zou, First-principle calculation of $\eta_c \to 2\gamma$ decay width from lattice QCD, arXiv:2109.09381.
[10] Y. Meng, A new method for a lattice calculation of $\eta_c \to 2\gamma$, Proc. Sci. LATTICE2021 (**2022**) 618 [arXiv:2110.05219].
[11] P. Vasko and J. Novotny, Two-loop QED radiative corrections to the decay $\pi^0 -> e^+e^-$: The virtual corrections and soft-photon bremsstrahlung, J. High Energy Phys. 10 (2011) 122.
[12] T. Husek, K. Kampf, and J. Novotný, Rare decay $\pi^0 \to e^+e^-$: On corrections beyond the leading order, Eur. Phys. J. C **74**, 3010 (2014).
[13] T. Blum, P. A. Boyle, T. Izubuchi, L. Jin, A. Jüttner, C. Lehner, K. Maltman, M. Marinkovic, A. Portelli, and M. Spraggs (RBC and UKQCD Collaborations), Calculation of the Hadronic Vacuum Polarization Disconnected Contribution to the Muon Anomalous Magnetic Moment, Phys. Rev. Lett. **116**, 232002 (2016).
[14] T. Blum *et al.* (RBC and UKQCD Collaborations), Domain wall QCD with physical quark masses, Phys. Rev. D **93**, 074505 (2016).
[15] This error-reduction strategy was independently suggested by P. Sanchez, P. Masjuan, and A. Soni (private communication).
[16] I. Larin *et al.* (PrimEx-II Collaboration), Precision measurement of the neutral pion lifetime, Science **368**, 506 (2020).
[17] X. Feng, S. Aoki, H. Fukaya, S. Hashimoto, T. Kaneko, J.-i. Noaki, and E. Shintani, Two-Photon Decay of the Neutral Pion in Lattice QCD, Phys. Rev. Lett. **109**, 182001 (2012).
[18] A. Gérardin, H. B. Meyer, and A. Nyffeler, Lattice calculation of the pion transition form factor with $N_f = 2 + 1$ Wilson quarks, Phys. Rev. D **100**, 034520 (2019).